Section: Radio-Diagnosis

Original Research Article

ROLE OF CONTRAST ENHANCED MULTIDETECTOR COMPUTED TOMOGRAPHY IN EVALUATION AND CHARACTERIZATION OF RETROPERITONEAL MASSES

Ashish Kumar Patel[1], Amlendu Nagar[2], Sheetal Singh[3], Bhushita Lakhkar Guru[4]

[1]3rd Year Junior Resident, Department of Radio-Diagnosis, Index Medical College Hospital and Research Centre, Indore, Madhya Pradesh, India.
[2]Professor & HOD, Department of Radio-Diagnosis, Index Medical College Hospital and Research Centre, Indore, Madhya Pradesh, India.
[3]Professor, Department of Radio-Diagnosis, Index Medical College Hospital and Research Centre, Indore, Madhya Pradesh, India.
[4]Professor, Department of Radio-Diagnosis, Index Medical College Hospital and Research Centre, Indore, Madhya Pradesh, India.

Received : *04/09/2024*
Received in revised form : *23/10/2024*
Accepted : *06/11/2024*

Corresponding Author:
Dr. Ashish Kumar Patel,
3rd Year Junior Resident, Department of Radio-Diagnosis, Index Medical College Hospital and Research Centre, Indore, Madhya Pradesh, India.
Email: ashishkumarpatel1995@gmail.com

DOI: 10.70034/ijmedph.2024.4.99

Source of Support: Nil,
Conflict of Interest: None declared

Int J Med Pub Health
2024; 14 (4); 524-433

ABSTRACT

Background: The retroperitoneal space is home to a variety of masses, which can be primary or secondary, neoplastic or non-neoplastic. Accurate diagnosis using imaging techniques is crucial for effective management. This study aims to evaluate the spectrum and characteristic imaging features of solid and cystic retroperitoneal masses using contrast-enhanced computed tomography (CECT), correlating these findings with histopathology.
Material and Methods: In this prospective cross-sectional study, 30 patients with suspected retroperitoneal masses underwent CECT. Imaging features were assessed, and results were correlated with pathological findings.
Results: This study involved patients aged 1 to 75 years, predominantly male (66.7%). Primary retroperitoneal masses made up 35.7% of cases, with lymphomas and liposarcomas being the most common types. Among secondary retroperitoneal masses, 42.1% were of pancreatic origin, followed by renal (31.6%), adrenal (21.1%), and aortic (5.2%) masses. Cystic lesions, primarily pancreatic pseudocysts, accounted for 30% of cases. In terms of vascularity, 43.3% of lesions were hypo- or non-vascular. Most lesions (66.6%) showed heterogeneous enhancement on CT scans. The overall accuracy of CT in diagnosis was 86.7%, with 84.6% accuracy for malignant lesions and 88.2% for non-malignant ones.
Conclusion: CECT is effective in evaluating retroperitoneal masses, providing valuable information for diagnosis and management. Characteristic imaging features, combined with clinical information, enhance diagnostic accuracy, aiding in differentiating between various types of lesions. The study underscores CT's effectiveness in differentiating between malignant and non-malignant retroperitoneal masses, making it a valuable tool for accurate diagnosis and management.
Keywords: Retroperitoneal masses, contrast-enhanced computed tomography, imaging features, histopathology, neoplastic lesions, vascularity, enhancement patterns.

INTRODUCTION

The retroperitoneal space is defined as the area between the peritoneum and the posterior wall of the abdominal cavity. It is bounded superiorly by the diaphragm, inferiorly by the pelvic brim, and laterally extends to the tips of the twelfth ribs.[1] Retroperitoneal masses represent a diverse group of lesions that originate in the retroperitoneal spaces.[2] Most tumors that arise in this compartment derive from major retroperitoneal organs such as the pancreas, kidneys, and adrenal glands. Other tumors may include lymphoma, sarcoma, rhabdomyosarcoma, as well as those arising from connective tissue, fat, fascia, and metastases.[3]

Primary retroperitoneal masses, which originate within the retroperitoneum but outside the major retroperitoneal organs, are rare and can be categorized into solid and cystic masses, each of which can be further divided into neoplastic and non-neoplastic types. Among primary retroperitoneal neoplasms, 70% to 80% are malignant, accounting for approximately 0.1% to 0.2% of all malignancies in the body.[4] While these tumors can affect individuals of any age, they are most commonly found in adults.[5]

Retroperitoneal masses can be classified as primary when they originate from tissues other than major organs like the kidneys, adrenal glands, pancreas, or bowel loops.[6] These masses can be further categorized as solid or cystic based on their appearance on imaging.[7] Solid tumors can be divided into four groups: mesenchymal, neural, germ cell, and lymphoproliferative, depending on their origin.[8]

Among cystic tumors, the most common types are lymphangioma and cystic mesothelioma.[8-10] There are also non-neoplastic lesions, primarily including retroperitoneal fibrosis, non-Langerhans histiocytosis, and extramedullary hematopoiesis. Advances in radiological and imaging techniques have significantly improved the accuracy of diagnosing retroperitoneal masses compared to previous years. Enhanced diagnostic tools like ultrasonography, computed tomography (CT) scans, and magnetic resonance imaging (MRI) allow for comprehensive visualization of mass lesions.[11]

The introduction of CT scans has greatly enhanced the ability to evaluate the relationship of neoplasms to surrounding structures and to detect lymph node metastases.[12] CT scans are among the most useful and widely accepted imaging techniques, providing accurate diagnoses for nearly all adrenal tumors. They are particularly effective in diagnosing pheochromocytoma and can delineate neuroblastomas while offering insights into potential invasion of adjacent tissues or organs.[13]

When investigating renal masses, the primary advantages of CT scanning include its ability to demonstrate direct extrarenal extension and venous involvement, identify small masses—especially anterior and posterior subcapsular masses when urograms are normal—and detect metastatic deposits in lymph nodes, liver, and lungs. In cases of cystic diseases, CT can reveal associated conditions in the liver and pancreas. Additionally, CT offers better resolution than ultrasound and is less dependent on the operator's skill.[14]

Carcinomas of the head or body of the pancreas are typically identified by CT scans as localized hypodense masses of variable attenuation that distort local anatomy. Tumor extension beyond the pancreas can be assessed with intravenous contrast infusion, which allows for the evaluation of encasement of adjacent vascular structures. The most reliable indicators of malignancy in the presence of a pancreatic mass include the detection of focal intrahepatic lesions and enlarged lymph nodes.[15]

The demonstration of a pseudocyst's extent and location in relation to adjacent organs is valuable preoperative information.[16] CT scans provide precise anatomical details regarding the size and position of retroperitoneal tumors, such as lymph node metastases, lymphomas, fibrosarcomas, rhabdomyosarcomas, and leiomyomas. They can accurately depict the extent of these tumors and their involvement with nearby organs.[11]

In our study, we aim to evaluate the spectrum and recognize the characteristic imaging features of various solid and cystic retroperitoneal masses using Contrast Enhanced Computed Tomography. We will correlate these findings with histopathology and therapeutic responses, ultimately aiding in accurate diagnosis and guiding further management.

Table 1: Classification of retroperitoneal masses

SOLID: NEOPLASTIC
Lymphoid tumors
Lymphoma
Sarcomas
Liposarcoma
Malignant fibrous histiocytoma
Leiomyosarcoma
Neurogenic tumors
Schwannoma
Paraganglioma
Ganglioneuroma
Neurofibroma
Immature teratoma
SOLID: NON-NEOPLASTIC
Retroperitoneal fibrosis
Extramedullary hematopoiesis
Erdheim-Chester disease
Cystic: Non-neoplastic
Lymphangiomas
Mullerian cysts
Epidermoid cyst
Pancreatic pseudocysts

Lymphoceles
Urinomas
Hematomas

MATERIALS AND METHODS

After receiving approval from the institutional ethical committee, this prospective cross-sectional study was conducted in the Department of Radiodiagnosis at Index Medical College Hospital and Research Centre, Indore. The study included 30 patients referred from various departments who presented with abdominal pain and nonspecific symptoms indicative of a retroperitoneal mass, undergoing Contrast Enhanced Computed Tomography (CECT) during the eight-month study period from July 1, 2023, to February 29, 2024. Patients satisfying the inclusion criteria were clearly informed about the purpose and nature of the study in a language they could understand, and written informed consent was obtained prior to their inclusion in the study.

Inclusion Criteria

- Patients with clinically suspected retroperitoneal masses who were referred for a Contrast Enhanced Computed Tomography (CECT) abdomen study during the study period were included.
- Patients who consented to participate in the study.

Exclusion Criteria

- Patients with lesions not located at the retroperitoneal region
- Patients who are not willing to give consent
- Pregnant female
- Elevated serum creatinine level >1.5mg/dl and urea >40mg/dl
- Patients with sensitivity to contrast agent (Allergic reactions)
- Patients with unstable general condition

Methodology

Patients with a clinical suspicion of retroperitoneal masses were initially evaluated using ultrasound of the abdomen. The ultrasound was performed with a 3 MHz convex transducer, utilizing acoustic gel for effective skin-to-transducer coupling. Following this, multi-slice CT scans of the abdomen and pelvis were conducted for further evaluation.

Computed tomography examination protocol design

CT scans were performed using a Siemens 128-slice multi-detector Healthineers Somatom Go Top machine. Contrast Enhanced Computed Tomography (CECT) of the abdomen and pelvis was conducted with both oral and intravenous contrast. A total of 100 ml of non-ionic iodinated contrast medium (iohexol, iodine concentration 300 mg/ml) was injected through an 18–20-gauge intravenous cannula at a rate of 3 ml/sec, followed by a 20 ml saline flush at 2 ml/sec. Scanning in the arterial phase was completed with a scan time of 20.5 seconds. After a 60-second interval post-contrast administration, venous phase scanning was performed, also with a scan time of 20.5 seconds.

Patient preparation for computed tomography examinations.

All patients were instructed to fast for 6 hours prior to the scan. They were asked to remove all metallic items, including zippers on pants, and provided with gowns to wear. An intravenous cannula was then inserted into the patient's arm for the administration of contrast.

Computed tomography images interpretation

The CT data were assessed by two experienced radiologists in consensus, with both observers remaining unaware of each patient's pathological information.

CT images

On CECT, the first step was to confirm that the mass was located in the retroperitoneal space, followed by an assessment of its definition, consistency, and components, such as fat, calcium, and necrosis. The pattern of enhancement was evaluated (whether unenhanced, homogeneous, or heterogeneous), along with the average CT attenuation measured in Hounsfield units (HU).

Sagittal and coronal reformations of the images were obtained using Maximum Intensity Projection (MIP), Minimum Intensity Projection (MRP), and Volume Rendering Technique (VRT). Both axial and reformatted coronal and sagittal images were carefully evaluated

The approach to evaluating abdominal or pelvic masses began with differentiating solid primary retroperitoneal masses based on their location, pattern of spread, vascularity, and composition. Cystic lesions were classified according to their site, specific imaging characteristics, and clinical history.

CT images interpretation

In each case, the CT imaging features of the lesions were interpreted as described, leading to either a most probable diagnosis, two differential diagnoses, multiple differential diagnoses, or an inconclusive diagnosis.

The results were subsequently correlated with the pathological data.

Standard of reference

All cases underwent pathological analysis through open surgical biopsy, surgical excision, or image-guided biopsy via CT or ultrasound. Pathological data served as the standard reference.

The findings were recorded on a pre-structured proforma for the study, and descriptive statistics were conducted to identify the characteristics of the collected data.

Statistical Analysis

Raw data were recorded in Excel and analyzed using IBM SPSS version 22.0. Continuous parametric data were summarized with mean and standard deviation, while non-parametric data were summarized using median and interquartile range. Categorical data were presented as percentages. The Chi-square test was utilized for comparing categorical data, and an independent t-test was employed for continuous data. A p-value under 0.05 indicated statistical significance.

RESULTS

On CT, the first step was to confirm the site as retroperitoneal and exclude any organ of origin. This was followed by an assessment of the lesion's definition, consistency, and components (such as fat, calcium, and necrosis). The pattern of enhancement was evaluated as unenhanced, homogeneous, or heterogeneous. Vascularity and average CT attenuation were assessed by measuring Hounsfield units (HU) in five different locations and calculating the average HU.

Out of the 30 cases, 11 (36.7%) were classified as primary retroperitoneal masses, while the remaining 19 (63.3%) were secondary retroperitoneal masses arising from retroperitoneal organs. [Table 1]

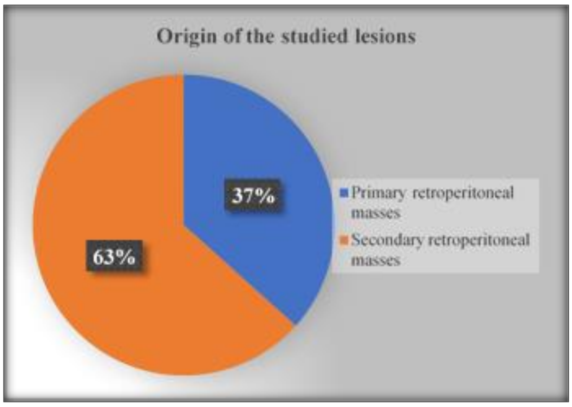

Figure 1: Distribution of patients based on Origin of the studied lesions

Among the 11 cases of primary retroperitoneal mass lesions, 8 (72.7%) were identified as neoplastic, while 3 (27.3%) were non-neoplastic. Within the neoplastic category, lymphoma was the most common type, representing 3 cases (27.3%), followed by liposarcoma, which accounted for 2 cases (18.1%). The sole non-neoplastic lesion was hematoma, also present in 3 cases (27.3%).

Among the 19 cases of secondary retroperitoneal masses, 8 (42.1%) were of pancreatic origin, 6 (31.6%) were of renal origin, 4 (21.1%) were of adrenal origin, and 1 (5.2%) case were of aortic origin. [Table 2]

Renal lesions included 3 cases of renal cell carcinoma (RCC), 1 case of oncocytoma, 1 case of Wilms tumor, and 1 case of angiomyolipoma. Of the 3 RCC cases, two exhibited the Embedded Organ sign, while one displayed both the Embedded Organ and Beak signs. Additionally, one case had distant metastasis.

Adrenal lesions comprised 1 cases of adenoma,1 case of myelolipoma, 1 case of metastasis, and 1 case of hematoma. The adrenal adenomas had a Hounsfield unit (HU) value of less than 10 and demonstrated a washout of greater than 60% on delayed imaging, consistent with typical findings of adrenal adenoma. Additionally, the adenomas exhibited the phantom sign.

In this study, tumors with paraspinal locations being the most common epicenter in 11 cases (36.7%). Displacement of adjacent organs occurred in 12 cases (40%), while infiltration into adjacent organs was noted in five cases (16.7%). Vascular encasement was detected in seven cases (23.3%), and distant metastasis was identified in six cases (20%). [Table 3]

Regarding consistency in the cystic lesions, there were nine (30%) purely cystic lesions, six (20%) mixed lesions, and fifteen (50%) solid lesions. Among the cystic lesions, pancreatic pseudocysts were the most common, making up 44.5% of cases (4 instances). Other less common cystic masses included psoas hematoma, teratoma, serous cystadenoma, mucinous cystadenoma, and adrenal hematoma, each accounting for 11.1% (1 case each). This demonstrates that pancreatic pseudocysts are significantly more prevalent than other cystic lesions in the retroperitoneum. [Table 4]

In terms of vascularity, only one lesion (3.3%), a paraganglioma was hyper-vascular. 13 (43.3%) lesions showed no or hypo-vascularity, including liposarcoma (3), schwannoma (1), lymphoma (4), mucinous cystadenoma (1), and pancreatic pseudocysts (4). The remaining 16 (53.4%) lesions had moderate vascularity, indicating that most lesions in the study had low vascularity. [Table 3]

Regarding lesion enhancement, five lesions were unenhanced, accounting for 16.7% of the total (1 schwannoma and 4 pancreatic pseudocysts). Five lesions showed homogeneous enhancement (16.7%), including 1 paraganglioma (markedly enhanced) and 4 lymphomas (mildly enhanced). The remaining lesions, comprising 66.6% of the total, exhibited heterogeneous enhancement. [Table 5]

In our study, we found that out of the 3 cases of lymphoma, all exhibited well-defined lobulated margins, with 75% showing the classic floating aorta sign and vascular encasement. On post-contrast imaging, all 3 cases (100%) demonstrated mild homogeneous enhancement, with no cases showing necrosis. The second most common mesodermal neoplasm identified was liposarcoma, accounting for 18.2%. Liposarcoma presented with thick, irregular, and nodular septa, and on post-contrast imaging, it exhibited enhancement. These characteristics are useful for differentiating liposarcoma from lipoma. [Table 6]

In our study two case diagnosed as primary retroperitoneal masses on CT were confirmed to be neurogenic tumors on histopathological examination. Among them one was schwannoma and one paraganglioma. The lesion diagnosed as schwannoma appeared as a well-defined homogenous mass in the paravertebral region and shows heterogenous enhancement on post contrast study. Paraganglioma was found as a large well-defined lobulated mass with haemorrhage and shows intense enhancement on post contrast.

In our study one case diagnosed as teratoma out of 11 primary retroperitoneal masses and shows features as complex mass that contained multiple well-circumscribed fluid components, fat, and calcification in a tooth like configuration.

In terms of diagnostic consistency with CT findings, 20 lesions (66.7%) were confirmed as consistent with the CT diagnosis. 6 lesions (26.7%) were identified as one of two differential diagnoses by CT. 2 lesion (6.6%) was categorized as one of more than two differential diagnoses, while two lesion (6.6%) was not included as a differential diagnosis or had no definite diagnosis by CT.

The diagnostic accuracy of contrast-enhanced computed tomography (CT) for retroperitoneal lesions was 86.7% overall. Specifically, it achieved 84.6% accuracy for malignant lesions and 88.2% for non- malignant lesions, demonstrating its effectiveness in differentiating between these types. [Table 7]

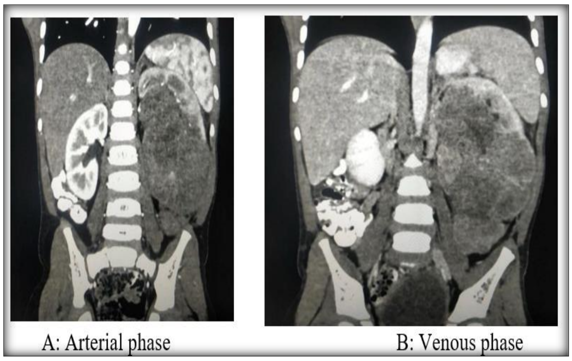

Figure 1: Case of renal cell carcinoma (Wilms Tumour). Contrast enhanced computed tomography scan of a 4-year-old child with retroperitoneal large heterogeneously enhancing hypodense solid lesion with multiple areas of necrosis is seen in left kidney. (A) Reformatted coronal image (arterial phase). (B) Reformatted coronal image (venous phase)

Figure 2: Case of retroperitoneal Lymphoma. Contrast enhanced computed tomography scan of a 40-year-old male patient with large pre-vertebral homogenous retroperitoneal soft tissue density mass lesion. Shows homogenous enhancement. It ensases the abdominal aorta. (A) Axial image. (B) Reformatted coronal image (C) Reformatted sagittal image

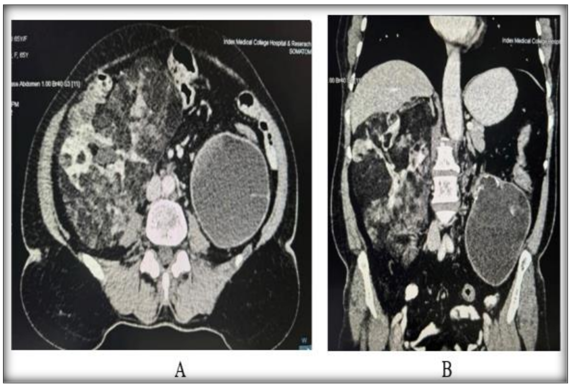

Figure 3: Case of Bilateral Renal angiomyolipoma. Contrast enhanced computed tomography scan of a 65-year-old female patient with mixed fat solid vascularized giant mass in the right and left renal space. (A) Axial image. (B) Reformatted coronal image

Figure 4: Case of bilateral adrenal myelolipoma. Contrast enhanced computed tomography scan of a 50-year-old male patient shows well defined lobulated heterogenous hypodense fat density lesion with enhancing soft tissue seen in bilateral adrenal gland. (A) Axial image. (B) Reformatted coronal image

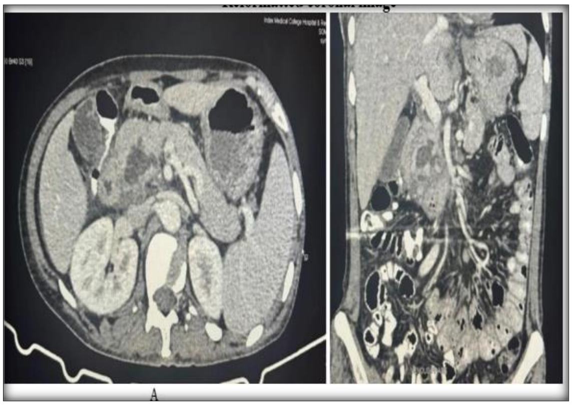

Figure 5: Case of serous cystadenoma of pancreas. Contrast enhanced computed tomography scan of a 40-year-old male patient shows multicystic lobulated mass in the pancreatic head. (A) Axial image. (B) Reformatted coronal image

Figure 6: Case of adrenal metastasis, this was a known case of carcinoma lung. Contrast enhanced computed tomography scan of a 70-year-old male patient shows well defined heterogeneous soft tissue density lesion seen in right adrenal gland. (A) Axial image. (B) Reformatted coronal image

Figure 7: Case of adrenal hematoma. Contrast enhanced computed tomography scan of a 20-year-old male patient shows ovoid hypodense mass in the right adrenal gland associated with liver laceration with stranding in the perirenal fat and a subcapsular collection in the right kidney. (A) Axial image. (B) Reformatted coronal image

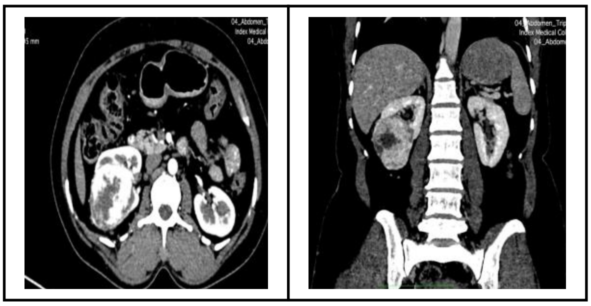

A **B**

Figure 8: Case of renal cell carcinoma (Oncocytoma). Contrast enhanced computed tomography scan of 56-year-old female patient with sharply circumscribed mass in right kidney demonstrate avid contrast uptake with hypodense star shaped central scar. (A) Axial image (cortico-medullary phase). (B) Reformatted coronal image (nephrogenic phase).

Table 2: Distribution of study population depending upon Primary Retroperitoneal mass spectrum

Primary Retropertitoneal Masses	Number	Frequency (%)
Lymphoma	3	27.3%
Liposarcoma	2	18.1%
Schwannoma	1	9.1%
Paraganglioma	1	9.1%
Teratoma	1	9.1%
Hematoma	3	27.3%
Total	11	100%

Table 3: Distribution of study population depending upon organ of origin

Organ of origin of retroperitoneal masses	Number	Frequency (%)
Pancreatic	8	42.1%
Renal	6	31.6%
Adrenal	4	21.1%
Aorta	1	5.2%
Total	19	100%

Table 4: Various imaging characteristics of retroperitoneal tumours

Characteristics of Retroperitoneal masses	Category	Number	Frequency (%)
Epicenter of tumour	Paraspinal spaces	11	36.7%
	Pararenal spaces	7	23.3%
	Pre and para-aortic region	7	23.3%
	Periampullary region	5	16.7%
Effect on adjacent structures			
Displacement of adjacent organ	Present	12	40%

	Absent	18	60%
Infiltration of adjacent organ	Present	5	16.7%
	Absent	25	83.3%
Vascular encasement	Present	7	23.3%
	Absent	23	76.7%
Distant metastases	Present	6	20%
	Absent	24	80%

Table 3: Distribution of study population depending upon Cystic retroperitoneal masses

Cystic retroperitoneal masses	Number	Frequency (%)
Pancreatic pseudocyst	4	44.5%
Psoas Hematoma	1	11.1
Teratoma	1	11.1
Serous cystadenoma pancreas	1	11.1
Mucinous cystadenoma pancreas	1	11.1
Adrenal hematoma	1	11.1
Total	9	100%

Table 4: Distribution of cystic lesions depending upon components of the computed tomography examined lesions

Component	Number	Frequency (%)
Fat	4	44.5%
Necrosis	1	11.1
Calcification	1	11.1
Haemorrhage	1	11.1
Total	9	100%

Table 5: Vascularity of the CT examined lesions

CT vascularity of the examined lesion	Number	Frequency (%)
No or Hypo	13	43.3%
Moderate	16	53.4%
Hyper	01	3.3%
Total	30	100%

Table 6: Enhancement of the CT examined lesions

CT enhancement of the examined lesion	Number	Frequency (%)
Unenhanced	05	16.7%
Homogenous	05	16.7%%
Heterogenous	20	66.6%
Total	30	100%

Table 7: Distribution of study population depending upon pathological diagnosis

Pathological diagnosis	Number	Frequency (%)
Non-neoplastic lesions (N=9)	**9**	**30%**
Pancreatic pseudo-cyst	4	44.5%
Renal hematoma	2	22.2%
Renal abscess	1	11.1%
Psoas Hematoma	1	11.1%
Adrenal hematoma	1	11.1%
Benign lesions (N=8)	**8**	**26.7%**
Adrenal myelolipoma	1	12.5%
Adrenal Adenoma	1	12.5%
Renal Angiomyolipoma	1	12.5%
Schwannoma	1	12.5%
Paraganglioma	1	12.5%
Teratoma	1	12.5%
Serous cystadenoma pancreas	1	12.5%
Mucinous cystadenoma pancreas	1	12.5%
Malignant lesions (n=13)	**13**	**43.3%**
Lymphoma	4	30.7%
Liposarcoma	3	23.1%
Renal cell carcinoma	3	23.1%
Pancreatic ductal adenocarcinoma	2	15.4%
Adrenal metastasis	1	7.7%

Table 8: Correlation Between Pathological and CT Imaging Diagnoses

Pathological diagnosis	Total (n=30)		Malignant (n=13)		Non-malignant (n=17)	
	No	%	No	%	No	%
Consistent with CT diagnosis	20	66.6	9	69.3	11	68.7
One of 2 differential diagnosis by CT	6	30	2	15.4	4	35.3

One of more than 2 differential diagnosis by CT	2	6.7	1	7.7	1	0.0

DISCUSSION

Contrast-enhanced MDCT scan is one of the most valuable and widely utilized imaging techniques for the evaluation of retroperitoneal tumors. It provides critical information on the tumor's location, origin, extent, composition (such as the presence of fat, calcification, or necrosis), enhancement patterns, and its interactions with nearby structures, including any distant metastases.[17] These specific imaging characteristics play an essential role in narrowing differential diagnoses and are crucial for developing an effective treatment plan. A retroperitoneal mass is typically diagnosed once its location within the retroperitoneum is confirmed, alongside the identification of its origin from a retroperitoneal organ. Despite the utility of MDCT in revealing key tumor features, radiologists often face diagnostic challenges, particularly in accurately localizing the lesion, determining its organ of origin, and assessing the extent of involvement.[18]

In this present study, 30 patients were subjected to contrast enhanced MDCT of abdomen. Patients with suspected retroperitoneal lesions were grouped under age, gender and contrast enhanced MDCT imaging patterns. In present study most were in the age group of 40-60 yrs. Male preponderance was observed in our study, with 20 males (66.7%) compared to 10 females (33.3%), resulting in a male-to- female ratio of 2:1. This finding aligns with the study conducted by Bhagat M et al., which similarly reported a higher prevalence of retroperitoneal tumors in males, particularly within the 40-60 years age group.[17]

Out of the 30 patients who were evaluated in our study, 11 cases (36.7%) were found to be primary retroperitoneal masses. The rest 19 cases (63.3%) were masses arising from retroperitoneal organs. Among the 11 cases of primary retroperitoneal mass lesions, 8 (72.7%) were identified as neoplastic, while 3 (27.3%) were non-neoplastic. Within the neoplastic category, lymphoma was the most common type, representing 3 cases (27.3%), followed by liposarcoma, which accounted for 2 cases (18.1%). The sole non-neoplastic lesion was hematoma, also present in 3 cases (27.3%).

In our study, we found that out of the 3 cases of lymphoma, all exhibited well-defined lobulated margins, with 75% showing the classic floating aorta sign and vascular encasement. On post-contrast imaging, all 3 cases (100%) demonstrated mild homogeneous enhancement, with no cases showing necrosis. The second most common mesodermal neoplasm identified was liposarcoma, accounting for 18. This was in concurrence with study done by Bhagat M et al,[17] and Rajiah et al.[19]

In our present study, the 2nd most common mesodermal neoplasm was liposarcoma, forming 18.1%. Liposarcoma showed thick, irregular, and nodular septa. On post contrast study, they showed enhancement. These features help in differentiating it from lipoma. This is consistent with the study done by Bhagat M et al,[17] and Rajiah et al.[19]

In our study, two cases initially diagnosed as primary retroperitoneal masses on CT were confirmed as neurogenic tumors through histopathological examination. These included one schwannoma and one paraganglioma. The schwannoma presented as a well-defined, homogenous mass in the paravertebral region with heterogeneous enhancement on post-contrast imaging. The paraganglioma appeared as a large, well-defined, lobulated mass with hemorrhage, displaying intense post-contrast enhancement. These findings are consistent with descriptions by Bhagat M et al. 17] and Rajiah et al.[19]

In our study, one of the 11 primary retroperitoneal masses was identified as a teratoma. Imaging revealed a complex mass characterized by multiple well-defined fluid components, fat, and calcifications arranged in a tooth-like configuration. These distinctive imaging features align closely with descriptions provided by Shin et al.[20] and Bhagat M et al.[18]

In our study, among the 19 cases of secondary retroperitoneal masses, 8 (42.1%) were of pancreatic origin, 6 (31.6%) were of renal origin, 4 (21.1%) were of adrenal origin, and 1 (5.2%) case were of aortic origin. Out of the 8 masses of pancreatic origin, 4 were of pseudocysts, 2 were of adenocarcinoma, 1 each of serous and mucinous cystadenomas. Pancreatic pseudocysts showed variable presentations with one of them showing splenic and portal vein thrombosis.

The renal lesions in our study included 3 cases of renal cell carcinoma (RCC), 1 case of oncocytoma, 1 case of Wilms tumor, and 1 case of angiomyolipoma. Among the 3 RCC cases, 2 exhibited the "embedded organ sign," while 1 case showed both the "embedded organ" and "beak" signs. One of the RCC cases also presented with distant metastasis. Adrenal lesions included 1 case of adenoma, 1 case of metastasis,1 case of hematoma, and 1 case of myelolipoma. The adrenal adenomas had Hounsfield unit (HU) values below 10 and demonstrated a washout of over 60% on delayed imaging, consistent with typical features of adrenal adenomas. Additionally, the adenomas displayed the "phantom sign." These imaging characteristics closely match the descriptions provided by Bhagat M et al.[17]

In our study, malignant lesions were more common than benign ones, aligning with observations from Chaudhari A et al,[8] and Stephens DH et al.[21] However, it is important to note that the study by Stephens DH et al. reported fewer benign cases than ours, largely because it included 10 recurrent cases, all classified as malignant, while our study did not feature any recurrent cases. Both studies underscore the critical role of CT in diagnosing retroperitoneal tumors and monitoring recurrences. Additionally, even in cases of advanced tumors, the insights provided by CT are invaluable for formulating an effective management strategy.

In this study, primary retroperitoneal masses accounted for 36.7% of cases, with 11 out of 30 instances. Among neoplastic masses, lymphoma emerged as the most common, comprising 3 cases (27.3%), followed by liposarcoma with 2 cases (18.1%). Hematoma, a non-neoplastic lesion, was also noted in 3 cases (27.3%). These findings align with studies by Bhagat M et al,[17] and Chinwan D et al,[21] which reported a prevalence of primary retroperitoneal masses at 33.3% and 43.3%, respectively. Bhagat M et al,[17] and Chaudhari et al,[8] identified lymphoma as the most common primary retroperitoneal mass, while Chinwan D et al,[21] reported lymph nodal masses accounting for 23%. The consistency in results may stem from similar sample sizes and comparable demographic characteristics in these studies.

In our study, we found that out of the 3 cases of lymphomas, all 3 had well defined lobulated margins, and majority of 66.6 % of them showed the classical floating aorta sign and vascular encasement. On post contrast study, 3 showed mild homogeneous enhancement. No one cases showed necrosis. which was consistent with findings of the study by Rajiah et al.[19]

The identification of fat and calcification in retroperitoneal tumors significantly narrows the differential diagnoses. In this study, four cases exhibited areas of fat attenuation within the lesion, with three being benign and one malignant. This suggests that fat is more commonly associated with benign lesions. A similar finding was noted in the study by Bosniak M et al,[22] which highlighted that angiomyolipoma could be diagnosed through the detection of fat in renal lesions, making fat the key radiologic feature that distinguishes angiomyolipoma from renal cell carcinoma (RCC). Additionally, adrenal adenomas and myelolipomas also displayed areas of fat attenuation, with the presence of significant intracellular cytoplasmic lipid serving as a crucial factor in differentiating benign from malignant adrenal tumors.[23]

The presence of necrosis, characterized by low attenuation and lack of contrast enhancement, is a critical indicator often associated with malignant tumors. In this study, necrosis was observed in 11 cases, with 10 being malignant and one benign cases, specifically pheochromocytoma and paraganglioma. Renal cell carcinoma (RCC) was identified as a hypodense lesion on non-enhanced scans, exhibiting heterogeneous post-contrast enhancement alongside central necrosis. Calcifications were noted in 33.3% of cases, and all RCC cases presented with necrosis. Similar observations were reported by Zagoria RJ et al,[24] who found calcifications in 31% and necrosis in 87.5% (7/8) of cases, and Hatimota P et al,[25] who indicated that necrosis was present in 94% of RCC cases.

Vascular encasement is a key feature of malignant tumors and is critical in evaluating their surgical resectability. In our study, only one lesion (3.3%), a paraganglioma, was found to be hypervascular. Thirteen lesions (43.3%) exhibited no or low vascularity, including cases of liposarcoma (3), schwannoma (1), lymphoma (4), mucinous cystadenoma (1), and pancreatic pseudocysts (4). The remaining 16 lesions (53.4%) demonstrated moderate vascularity, suggesting that the majority of the tumors had low vascularity. These results are consistent with the findings of Lee ES et al,[26] who emphasized the utility of multidetector CT in evaluating vascular involvement, a crucial determinant in assessing tumor resectability.

In our study, the diagnostic accuracy of contrast-enhanced computed tomography (CT) for retroperitoneal lesions was 86.7% overall. Specifically, it achieved 84.6% accuracy for malignant lesions and 88.2% for non-malignant lesions, demonstrating its effectiveness in differentiating between these types. These findings are consistent with the study conducted by Anwar D et al., which reported that CT imaging had an overall diagnostic accuracy of 88.1%. Specifically, it demonstrated 100% accuracy in diagnosing non-malignant lesions and 80.8% accuracy in identifying malignant lesions.[18]

Our findings align with those of Shalaan,[27] who reported a 74% accuracy rate for CT in diagnosing retroperitoneal lesions, using a similar diagnostic approach. In Shalaan's study, CT accurately identified positive cases in 37 out of 50 patients and negative cases in 13. This is further supported by Küster et al,[28] who conducted CT examinations on 287 patients and concluded that CT should be the primary diagnostic tool for staging retroperitoneal tumors and identifying recurrences, with an overall accuracy of 90%. Additionally, Neifeld et al,[29] studied 21 patients with retroperitoneal sarcomas and found that CT provided accurate results in 18 cases, with only three misleading diagnoses. The study also highlighted CT's value in detecting tumor recurrence and assessing chemotherapy response through follow-up scans.

The limitations of this study include a small sample size and the inability to conduct histopathological examinations in four cases involving adrenal lesions. Additionally, the case diagnosed as pheochromocytoma via CT was not subjected to biopsy due to the potential risk of triggering a hypertensive crisis.

CONCLUSION

In conclusion, our findings indicate that multidetector computed tomography (MDCT) demonstrates high accuracy in diagnosing and detecting retroperitoneal masses. With 66.7% of cases confirmed as consistent diagnoses, MDCT achieved an overall accuracy of 86.7%, specifically 84.6% for malignant lesions and 88.2% for non-malignant lesions. These results underscore the effectiveness of MDCT in differentiating between malignant and non-malignant masses. Furthermore, MDCT is the most accurate radiological modality for the early diagnosis, characterization, and differentiation of retroperitoneal masses, reinforcing its essential role in guiding timely and appropriate clinical management.

REFERENCES

1. Selçuk İ, Ersak B, Tatar İ, Güngör T, Huri E. Basic clinical retroperitoneal anatomy for pelvic surgeons. Turk J Obstet Gynecol. 2018 Dec;15(4):259-269.
2. Nishino M, Hayakawa K, Minami M, Yamamoto A, Ueda H, Takasu K. Primary retroperitoneal neoplasms: CT and MR imaging findings with anatomic and pathologic diagnostic clues. Radiographics. 2003 Jan-Feb;23(1):45-57.
3. Strauss DC, Hayes AJ, Thomas JM. Retroperitoneal tumours: review of management. Ann R Coll Surg Engl. 2011 May;93(4):275-80.
4. Neville A, Herts BR. CT characteristics of primary retroperitoneal neoplasms. Crit Rev Comput Tomogr. 2004;45(4):247-70.
5. Goenka AH, Shah SN, Remer EM. Imaging of the retroperitoneum. Radiol Clin North Am. 2012 Mar;50(2):333-55
6. Tiu A, Sovani V, Khan N, Hooda S. Primary retroperitoneal mature cystic teratoma (dermoid cyst) in a 51-year-old male:Case report and historical literature review. SAGE Open Med Case Rep. 2017 Mar 23; 5:2050313X17700745.
7. Scali EP, Chandler TM, Heffernan EJ, Coyle J, Harris AC, Chang SD. Primary retroperitoneal masses: what is the differential diagnosis? Abdom Imaging. 2015 Aug;40(6):1887-903.
8. Chaudhari A, Desai PD, Vadel MK, Kaptan K. Evaluation of primary retroperitoneal masses by computed tomography scan. Int J Med Sci Public Health. 2016; 5:1423-29.
9. Lo YS, Wang JS, Yu CC, Chou CP, Chen CJ, Lin SL, Lee MG, Kuo YC, Tseng HH. Retroperitoneal enteric duplication cyst. J Chin Med Assoc. 2004 Sep;67(9):479-82.
10. Ayyappan AP, Jhaveri KS, Haider MA. Radiological assessment of mesenteric and retroperitoneal cysts in adults: is there a role for chemical shift MRI? Clin Imaging. 2011 Mar- Apr;35(2):127-32
11. Mota MMDS, Bezerra ROF, Garcia MRT. Practical approach to primary retroperitoneal masses in adults. Radiol Bras. 2018 Nov-Dec;51(6):391-400.
12. Occhipinti M, Heidinger BH, Franquet E, Eisenberg RL, Bankier AA. Imaging the posterior mediastinum: a multimodality approach. Diagn Interv Radiol. 2015 Jul-Aug;21(4):293-306.
13. Albano D, Agnello F, Midiri F, Pecoraro G, Bruno A, Alongi P, Toia P, Di Buono G, Agrusa A, Sconfienza LM, Pardo S, La Grutta L, Midiri M, Galia M. Imaging features of adrenal masses. Insights Imaging. 2019 Jan 25;10(1):1.
14. Mittal MK, Sureka B. Solid renal masses in adults. Indian J Radiol Imaging. 2016 Oct- Dec;26(4):429-442.
15. Lee ES, Lee JM. Imaging diagnosis of pancreatic cancer: a state-of-the-art review. World J Gastroenterol. 2014 Jun 28;20(24):7864-77.
16. Aghdassi AA, Mayerle J, Kraft M, Sielenkämper AW, Heidecke CD, Lerch MM. Pancreatic pseudocysts--when and how to treat? HPB (Oxford). 2006;8(6):432-41
17. Maniesh Bhagat & Rajesh Kumar. Assessment of Contrast Enhanced Multidetector Computed Tomography in Diagnosis of Retroperitoneal Lesions. Sch J App Med Sci, 2023 Jan 11(1): 175-180.
18. Anwar, D., M. Abdelhay, R. The Role of Multidetector Computed Tomography in Characterization and Differentiation of Retroperitoneal Masses. Zagazig University Medical Journal, 2023; 525 -531.
19. Rajiah, P., Sinha, R., Cuevas, C., Dubinsky, T. J., Bush Jr, W. H., & Kolokythas, O. (2011). Imaging of uncommon retroperitoneal masses. Radiographics, 31(4), 949-976.
20. Shin, N. Y., Kim, M. J., Chung, J. J., Chung, Y. E., Choi, J. Y., & Park, Y. N. (2010). The differential imaging features of fat-containing tumors in the peritoneal cavity and retroperitoneum: the radiologic-pathologic correlation. Korean journal of Radiology, 11(3), 333-345
21. Chinwan D, Vohra P. Role of multidetector computed tomography in evaluation of retroperitoneal masses. Int J Res Med Sci. 2018;6(12):3949-53.
22. Bosniak M, Megibow A, Hulnick D, Horii S, Raghavendra B. CT diagnosis of renal angiomyolipoma: The importance of detecting small amounts of fat. Am J Roentgenol. 1988;151(3):497-501.
23. Korobkin M, Brodeur FJ, Yutzy GG, Francis IR, Quint LE, Dunnick NR, et al. Differentiation of adrenal adenomas from non-adenomas using CT attenuation values. AJR Am J Roentgenol. 1996;166(3):531-36.
24. Zagoria RJ, Wolfman NT, Karstaedt N, Hinn GC, Dyer RB, Chen YM. CT features of renal cell carcinoma with emphasis on relation to tumour size. Invest Radiol. 1990;25(3):261-66
25. Hatimota P, Vashist S, Aggarwal K, Kapoor A, Gupta NP. Spectrum of US and CT findings in renal neoplasms with pathologic correlation. Indian J Radiol Imaging. 2005;15(1):117.
26. Lee ES, Lee JM. Imaging diagnosis of pancreatic cancer: A state-of-the-art review. World J Gastroenterol WJG. 2014;20(24):7864-77.
27. Shalaan AEM, Medhat Refaat, Hesham Farouk and Gamal Saleh Saleh. The role of multi-slice CT in the characterization of different retroperitoneal masses. M.D. Thesis, Benha University, Faculty of Medicine 2017.
28. Küster W, Imhof H, Aiginger P,Kuber W, Latal D and Wittich G.Clinical and diagnostic value of computed tomography in retroperitoneal spaceoccupying extrarenal and extrapancreatic lesions. Wien klinWochenschr1981;93(9):275-280.
29. Neifeld JP, Walsh JW and Lawrence W. Computed tomography in the management of soft tissue tumors. Surgery, gynecology & obstetrics 2005;155(4):535-540.